J|A|C|S
ARTICLES

# Nanoscale Ln(III)-Carboxylate Coordination Polymers (Ln = Gd, Eu, Yb): Temperature-Controlled Guest Encapsulation and Light Harvesting

Xuanjun Zhang,[†] Mohamed Ali Ballem,[‡] Maria Ahrén,[†] Anke Suska,[§]
Peder Bergman,[||] and Kajsa Uvdal[*,†]

*Divisions of Molecular Surface Physics and Nanoscience, Nanostructured Materials, Applied Physics, and Semiconductor Materials, Department of Physics, Chemistry, and Biology, Linköping University, 581 83 Linköping, Sweden*

Received March 18, 2010; E-mail: kajsa@ifm.liu.se

***Abstract:*** We report the self-assembly of stable nanoscale coordination polymers (NCPs), which exhibit temperature-controlled guest encapsulation and release, as well as an efficient light-harvesting property. NCPs are obtained by coordination-directed organization of $\pi$-conjugated dicarboxylate (**L1**) and lanthanide metal ions Gd(III), Eu(III), and Yb(III) in a DMF system. Guest molecules *trans*-4-styryl-1-methylpyridiniumiodide (**D1**) and methylene blue (**D2**) can be encapsulated into NCPs, and the loading amounts can be controlled by changing reaction temperatures. Small angle X-ray diffraction (SAXRD) results reveal that the self-assembled discus-like NCPs exhibit long-range ordered structures, which remain unchanged after guest encapsulations. Experimental results reveal that the negatively charged local environment around the metal connector is the driving force for the encapsulation of cationic guests. The **D1** molecules encapsulated in NCPs at 140 °C can be released gradually at room temperature in DMF. Guest-loaded NCPs exhibit efficient light harvesting with energy transfer from the framework to the guest **D1** molecule, which is studied by photoluminescence and fluorescence lifetime decays. This coordination−directed encapsulation approach is general and should be extended to the fabrication of a wide range of multifunctional nanomaterials.

## Introduction

The coordination polymers (aka metal−organic frameworks, MOFs) have rapidly gained growing attention due to the structure diversity and characteristics for a number of practical applications, such as catalysis,[1] gas storage,[2] chiral transfer,[3] luminescence,[4] and nonlinear optics.[5] However, the macroscopic solid state nature of such materials show limited solution-based behavior, which hinders further applications. Recently, scaling down these materials has afforded an exciting new class of highly tailorable materials known as nanoscale coordination polymers (NCPs) or infinite coordination polymer particles (ICPs).[6−12] Compared with bulk coordination polymers, these promising nanomaterials exhibit new possibilities for solution-based applications, such as ion exchange,[7] multimodal bioimaging,[9] drug delivery,[10] and sensing.[10b] Very recently, dye molecules, peptide polymers, drugs, and small nanoparticles have been loaded into NCPs by coordination-directed self-assembly[12,13] and by elegant postsynthetic modifications.[10c] This combination of inorganic and organic or even bioactive components into single NCPs has made accessible an immense new area of materials science that has extraordinary implications in the development of multifunctional materials. However, the groundwork for this emerging field has been laid only in the past few

---

[†] Division of Molecular Surface Physics and Nanoscience.

[‡] Division of Nanostructured Materials.

[§] Division of Applied Physics.

[||] Division of Semiconductor Materials.

(1) (a) Ma, L.; Abney, C.; Lin, W. *Chem. Soc. Rev.* **2009**, *38*, 1248. (b) Farrusseng, D.; Aguado, S.; Pinel, C. *Angew. Chem., Int. Ed.* **2009**, *48*, 7502.

(2) (a) Phan, A.; Doonan, C. J.; Uribe-Romo, F. J.; Knobler, C. B.; O'keeffe, M.; Yaghi, O. M. *Acc. Chem. Res.* **2010**, *43*, 58. (b) Han, S. S.; Mendoza-Cortés, J. L.; Goddard, W. A., III. *Chem. Soc. Rev.* **2009**, *38*, 1460.

(3) Crassous, J. *Chem. Soc. Rev.* **2009**, *38*, 830.

(4) Allendorf, M. D.; Bauer, C. A.; Bhakta, R. K.; Houk, R. J. T. *Chem. Soc. Rev.* **2009**, *38*, 1330.

(5) Evans, O. R.; Lin, W. *Acc. Chem. Res.* **2002**, *35*, 511.

(6) See recent reviews: (a) Lin, W.; Rieter, W. J.; Taylor, K. M. L. *Angew. Chem., Int. Ed.* **2009**, *48*, 650. (b) Spokoyny, A. M.; Kim, D.; Sumrein, A.; Mirkin, C. A. *Chem. Soc. Rev.* **2009**, *38*, 1218. (c) Wang, X.; McHale, R. *Macromol. Rapid Commun.* **2010**, *31*, 331.

(7) (a) Oh, M.; Mirkin, C. A. *Nature* **2005**, *438*, 651. (b) Oh, M.; Mirkin, C. A. *Angew. Chem., Int. Ed.* **2006**, *45*, 5492.

(8) (a) Farha, O. K.; Spokoyny, A. M.; Mulfort, K. L.; Galli, S.; Hupp, J. T.; Mirkin, C. A. *Small* **2009**, *5*, 1727. (b) Jeon, Y.-M.; Armatas, G. S.; Kim, D.; Kanatzidis, M. G.; Mirkin, C. A. *Small* **2009**, *5*, 46. (c) Tanaka, D.; Henke, A.; Albrecht, K.; Moeller, M.; Nakagawa, K.; Kitagawa, S.; Groll, J. *Nat. Chem.* **2010**, *2*, 410. (d) Aimé, C.; Nishiyabu, R.; Gondo, R.; Kimizuka, N. *Chem.*−*Eur. J.* **2010**, *16*, 3604.

(9) (a) Taylor, K. M. L.; Rieter, W. J.; Lin, W. *J. Am. Chem. Soc.* **2008**, *130*, 14358. (b) Rieter, W. J.; Taylor, K. M. L.; An, H.; Lin, W.; Lin, W. *J. Am. Chem. Soc.* **2006**, *128*, 9024. (c) Taylor, K. M. L.; Jin, A.; Lin, W. *Angew. Chem., Int. Ed* **2009**, *47*, 7722. (d) deKrafft, K. E.; Xie, Z.; Cao, G.; Tran, S.; Ma, L.; Zhou, O. Z.; Lin, W. *Angew. Chem., Int. Ed.* **2009**, *48*, 9901.

(10) (a) Rieter, W. J.; Pott, K. M.; Taylor, K. M. L.; Lin, W. *J. Am. Chem. Soc.* **2008**, *130*, 11584. (b) Rieter, W. J.; Taylor, K. M. L.; Lin, W. *J. Am. Chem. Soc.* **2007**, *129*, 9852. (c) Taylor-Pashow, K. M. L.; Rocca, J. D.; Xie, Z.; Tran, S.; Lin, W. *J. Am. Chem. Soc.* **2009**, *131*, 14261.

***Scheme 1.*** Molecular Structures of Ligand **L1** and Guests Encapsulated in NCPs

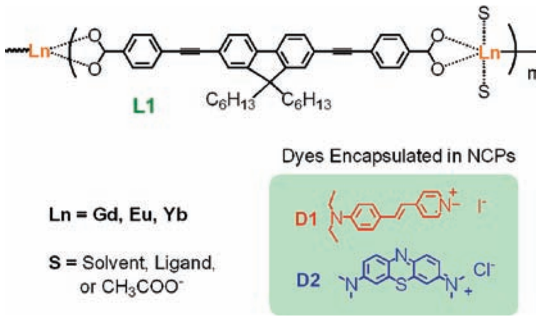

years. Hitherto, methods for controlling particle size and shape are still fairly rudimentary.[6b] Issues like porosity control and functional guest encapsulation and release have great potential in the areas of drug delivery, medical diagnostics, and materials science but pose a great challenge. This is to a large extent owing to different molecular forces in the precursor solution and general liability of the metal coordination numbers and geometries, which make it very challenging to control hierarchical assemblies through a preferred packing of the building blocks to give morphological and functional NCPs.

In this work, we report NCPs assembled from linear $\pi$-conjugated ligand and lanthanide metal ions (Scheme 1) with long-range ordered structures, which exhibit temperature-controlled sizing, guest encapsulation and release, and an efficient light-harvesting property. Fluorene derivatives are known for exhibiting high fluorescence quantum yields and excellent photostability.[14] $\pi$-Conjugated dicarboxylate ligand **L1** based on fluorene was synthesized by Sonogashira coupling, which exhibits strong blue photoluminescence. We choose lanthanide ions as metal connectors because of their high affinity to carboxylate and nondetrimental nature to fluorescence. The flexible coordination of lanthanide ions is expected to favor the adaptive encapsulations of guests in the coordination polymers.[8d,13]

It is well-known that solvent molecules or small anions always bind to metal ions when the main ligand cannot saturate the high coordination number of lanthanide ions.[15−17] If some anions (such as $CH_3COO^-$, etc.) bind to the empty orbitals of lanthanide ions in a neutral coordination polymer, the local environment around Ln(III) will be negatively charged and cationic guests are expected to balance the charges, leading to their encapsulation in NCPs. To test this hypothesis, NCPs derived from **L1** and Ln(III) (Ln = Gd, Eu, Yb) were prepared and the encapsulations of cationic guests were investigated. We choose *trans*-4-styryl-1-methylpyridiniumiodide (**D1**) and methylene blue (**D2**) as guests, which are important fluorophores in nonlinear optics and/or indicators in bioanalysis.[18]

## Results and Discussions

**Self-Assembly and Characterization of Ln(III)−L1 NCPs.** Bare NCPs derived from the **L1** and lanthanide ions without guest encapsulation in the form of nanoparticles were initially investigated. Here, we use **L1** and Gd(III) as an example to show the coordination-directed assembly of NCPs. With slow addition of $Gd(OAc)_3$ into a DMF solution of **L1**, the mixture turned turbid gradually and colloids exhibiting bright blue fluorescence formed after gentle stirring at room temperature for 20 min. SEM analysis revealed that the particles were relatively uniform disks with diameters of ca. 80−120 nm and thicknesses of ca. 10−20 nm (Figure 1a). The NCPs colloid (hereafter referred to as Gd−**L1**) was very stable. The material was stored at room temperature for several months, and no precipitate was observed. The solvent played a significant role in the self-assembly process, and DMF was found as a good medium for the stabilization of Gd−**L1** NCPs. When DMSO was used instead of DMF, aggregated spherical particles precipitated rapidly. This may indicate that DMF acts as stabilizer of the colloid particles. The presence of a coordinated DMF molecule was further confirmed by an IR spectrum (Supporting Information, Figure S1). The stretching mode $\nu$(C=O) of coordinated DMF in Gd−**L1** NCPs peaked at 1659 $cm^{-1}$. A shift of 13 $cm^{-1}$ toward a lower wavelength number compared with that of a free DMF molecule (1672 $cm^{-1}$) is a result of −C=O···Gd binding.[19] Thermogravimetric analysis (TGA) showed a weight loss of ca. 6% from 50 to 400 °C, followed by framework combustion (Figure S2). From these results and elemental analysis, we can obtain a composition of Gd $(\mathbf{L1})_{1.5}\cdot DMF\cdot H_2O$ for the NCPs.

For the reaction performed at 20 °C, the particles maintain diameters of ca. 80−120 nm after 20 min without further growth. Increasing the temperature could result in larger particles with a smoother surface, which likely is due to crystallization of the coordination polymer at higher temperature. In addition, the particle sizes could be tuned by changing the reaction time at elevated temperatures. For example, discus-like NCPs (with a thicker center and thinner edge) of 200−300 nm or 500−600 nm in diameters (Figure 1b and 1c) were obtained at 140 °C with a reaction time of 5 and 20 min, respectively, while other conditions remained unchanged (the particle growth could be quenched by addition of cold ethanol).

---

(11) (a) Imaz, I.; Rubio-Martínez, M.; Saletra, W. J.; Amabilino, D. B.; Maspoch, D. *J. Am. Chem. Soc.* **2009**, *131*, 18222. (b) Batabyal, S. K.; Peedikakkal, A. M. P.; Ramakrishna, S.; Sow, C. H.; Vittal, J. J. *Macromol. Rapid Commun.* **2009**, *30*, 1356. (c) Larionova, J.; Guari, Y.; Sangregorio, C.; Guérin, C. *New J. Chem.* **2009**, *33*, 1177. (d) Kerbellec, N.; Catala, L.; Daiguebonne, C.; Gloter, A.; Stephan, O.; Bünzli, J.-C.; Guillou, O.; Mallah, T. *New J. Chem.* **2008**, *32*, 584. (e) Maeda, H.; Hasegawa, M.; Hashimoto, T.; Kakimoto, T.; Nishio, S.; Nakanishi, T. *J. Am. Chem. Soc.* **2006**, *128*, 10024. (f) Sun, X.; Dong, S.; Wang, E. *J. Am. Chem. Soc.* **2005**, *127*, 13102.

(12) (a) Yan, Y.; Martens, A. A.; Besseling, N. A. M.; de Wolf, F. A.; de Keizer, A.; Drechsler, M.; Stuart, M. A. C. *Angew. Chem., Int. Ed.* **2008**, *47*, 4192. (b) Imaz, I.; Hernando, J.; Ruiz-Molina, D.; Maspoch, D. *Angew. Chem., Int. Ed.* **2009**, *48*, 2325. (c) Champness, N. R. *Angew. Chem., Int. Ed.* **2009**, *48*, 2274. (d) Zhang, X.; Chen, Z.-K.; Loh, K. P. *J. Am. Chem. Soc.* **2009**, *131*, 7210.

(13) (a) Nishiyabu, R.; et al. *J. Am. Chem. Soc.* **2009**, *131*, 2151. (b) Nishiyabu, R.; Aimé, C.; Gondo, R.; Noguchi, T.; Kimizuka, N. *Angew. Chem., Int. Ed.* **2009**, *48*, 9465.

(14) (a) Belfield, K. D.; Bondar, M. V.; Przhonska, O. V.; Schafer, K. J. *J. Photochem. Photobiol., A* **2004**, *162*, 489. (b) Yao, S.; Schafer-Hales, K. J.; Belfield, K. D. *Org. Lett.* **2007**, *9*, 5645.

(15) Bünzli, J.-C. G. *Coordination Chemistry of the Trivalent Lanthanide Ions: An Introductory Overview. In Rare Earths*; Saez Puche, R., Caro, P., Eds.; Editorial Complutense: Madrid, Spain, 1998.

(16) (a) Bünzli, J.-C. G. *Acc. Chem. Res.* **2006**, *39*, 53. (b) Bünzli, J.-C. G.; Piguet, C. *Chem. Rev.* **2002**, *102*, 1897.

(17) (a) Long, D.-L.; Blake, A. J.; Champness, N. R.; Wilson, C.; Schröder, M. *Chem.*−*Eur. J.* **2002**, *8*, 2026. (b) Hill, R. J.; Long, D.-L.; Champness, N. R.; Hubberstey, P.; Schröder, M. *Acc. Chem. Res.* **2005**, *38*, 337.

(18) (a) He, G. S.; Tan, L.-S.; Zheng, Q.; Prasad, P. N. *Chem. Rev.* **2008**, *108*, 1245. (b) Kono, M.; Kondo, T.; Takagi, Y.; Wada, A.; Fujimoto, K. *Clin. Chim. Acta* **2009**, *404*, 105.

(19) (a) Tian, H.-Y.; Zhang, G.; Wang, M.-C.; Li, X.-Y.; Wang, M. *Chin. J. Energet. Mater.* **2009**, *17*, 541. (b) MacNeill, C. M.; Day, C. S.; Gamboa, S. A.; Lachgar, A.; Noftle, R. E. *J. Chem. Crystallogr* **2010**, *40*, 222.

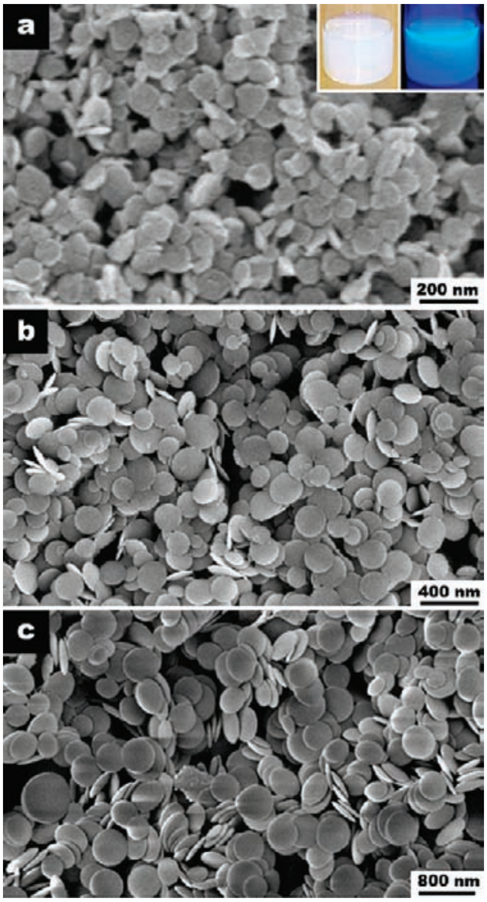

***Figure 1.*** SEM images of Gd−**L1** NCPs prepared in DMF at different reaction conditions: (a) 20 °C for 20 min; (b) 140 °C for 5 min; (c) 140 °C for 20 min. Inset in (a): photo images of Gd−**L1** NCPs under daylight and UV shine.

This approach to stable NCPs colloids can be extended to the synthesis of NCPs with other lanthanide ions such as Eu(III) and Yb(III) in a DMF system. Figure 2 showed the SEM and TEM images of Eu−**L1** and Yb−**L1** NCPs prepared at 140 °C. It is noted that all of these NCPs exhibit a discus-like morphology, which likely resulted from a preferred arrangement of the building blocks. Therefore, small-angle X-ray diffraction (SAXRD) was performed to study this interesting self-assembled nanostructure. The discus NCPs (Gd−**L1**, Eu−**L1**, and Yb−**L1**) exhibit long-range ordered structures, as revealed by the reflections in the $2\theta$ range from 2° to 10° shown in Figure 3. The *d*-spacing of the reflections and lattice constants calculated from the SAXRD data were summarized in Table 1.[20] The sequence of reflections with relative positions 1, $\sqrt{3}$, $\sqrt{4}$ is characteristic for a hexagonal structure.[21]

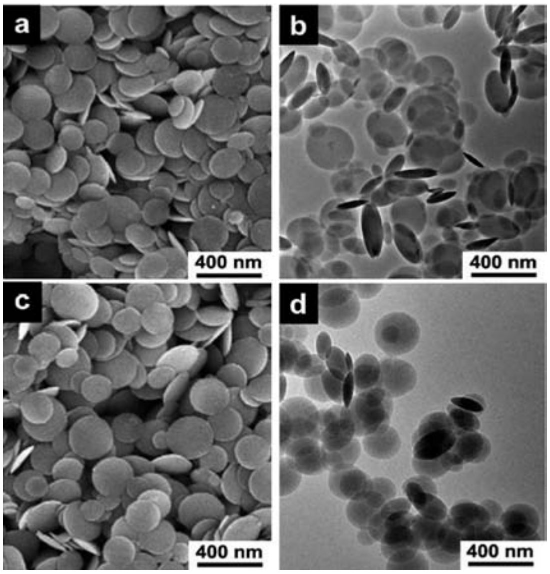

***Figure 2.*** SEM and TEM images of Eu−**L1** and Yb−**L1** NCPs prepared at 140 °C (10 min reaction): (a) SEM image of Eu−**L1**; (b) TEM image of Eu−**L1**; (c) SEM image of Yb−**L1**; (d) TEM image of Yb−**L1**.

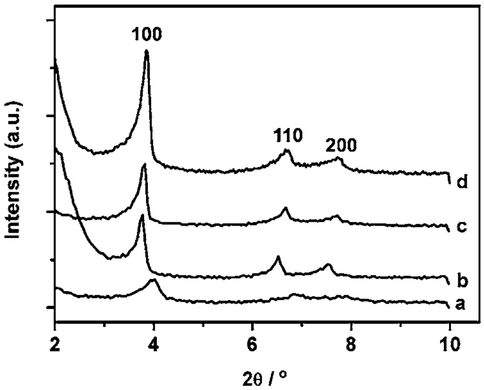

***Figure 3.*** Small angle X-ray diffraction (SAXRD) data: (a) Gd−**L1** prepared at 20 °C; (b) Gd−**L1** prepared at 140 °C; (c) Eu−**L1** prepared at 140 °C; (d) Yb−**L1** prepared at 140 °C.

**Temperature-Controlled Guest Encapsulations.** As anticipated, the NCPs can encapsulate functional species. For example, **D1**-loaded NCPs could be obtained by addition of $Gd(OAc)_3$ into the solution containing ligand **L1** and **D1** in DMF via a one-step coordination-directed assembly process. However, the guest loading amount was low (<1 mol % compared with **L1**) at room temperature. Considering the stable colloids of bare Gd−**L1** NCPs formed in DMF, we reasoned that some DMF molecules binding to Gd(III) might interfere with the coordination of acetate anions. As a solvent, DMF is expected to lose (or reduce) the competitive strength of coordination at elevated temperatures. Experimental results showed that the guest loading amount increased with an increase of the temperature from 20 to 140 °C. As shown in Figure 4, by normalizing the absorption peak that resulted from **L1**, the peak of **D1** in NCPs at ~480 nm increased apparently for the sample prepared at 140 °C. This was further supported by the color changes of the samples after purification (Figure 4, inset). The shoulder band of **L1** that arises after encapsulation of **D1** is most likely a result of the slight aggregation of the particles. Since there is a long tail of the absorption curve in the visible region, which is attributed

---

(20) If *a* is the lattice constant, the Bragg spacing of the first three orders of reflection from the hexagonal packing pattern should be as follows: $d_{100} = \sqrt{3}a/2$, $d_{110} = a/2$, $d_{200} = \sqrt{3}a/4$; or $d_{100}:d_{110}:d_{200} = 1:0.577:0.5$.

(21) (a) Tchebotareva, N.; Yin, X.; Watson, M. D.; Samorì, P.; Rabe, J. P.; Müllen, K. *J. Am. Chem. Soc.* **2003**, *125*, 9734. (b) Chandrasekhar, S.; Sadashiva, B. K.; Suresh, K. A. *Pramana* **1977**, *9*, 471. (c) Donnio, B.; Heinrich, B.; Gulik-Krzywicki, T.; Delacroix, H.; Guillon, D.; Bruce, D. W. *Chem. Mater.* **1997**, *9*, 2951. (d) Terazzi, E.; Bénech, J. M.; Rivera, J. P.; Bernardinelli, G.; Donnio, B.; Guillon, D.; Piguet, C. *Dalton* **2003**, 769. (e) Manickam, M.; Belloni, M.; Kumar, S.; Varshney, S. K.; Rao, D. S. S.; Ashton, P. R.; Preece, J. A.; Spencer, N. *J. Mater. Chem.* **2001**, *11*, 2790.

*Table 1.* SAXRD Data of the NCPs Prepared at 20 °C (Denoted with *) and 140 °C

| | Gd−**L1*** | Gd−**L1** | Eu−**L1** | Yb−**L1** | Gd−**L1**−**D1** |
|---|---|---|---|---|---|
| $d_{100}$/nm | 2.25 | 2.34 | 2.31 | 2.30 | 2.28 |
| $d_{110}$/nm | 1.29 | 1.35 | 1.32 | 1.33 | 1.31 |
| $d_{200}$/nm | 1.13 | 1.17 | 1.15 | 1.15 | 1.15 |
| Lattice constant ($a$)/nm | 2.60 | 2.70 | 2.67 | 2.66 | 2.63 |
| $d_{100}$:$d_{110}$:$d_{200}$ | 1:0.573:0.502 | 1:0.578:0.5 | 1:0.571:0.498 | 1:0.578:0.5 | 1:0.575:0.504 |

to Mie scattering caused by nanosized particles,[22] a more accurate loading amount was determined by UV−vis absorptions (taking extinction coefficients into account) after digesting Gd−**L1**−**D1** NCPs using acetic acid. The **D1** loading amount based on **L1** at 140 °C is ~6.7 mol %, while that at 20 °C is less than 1 mol %. This is, to our knowledge, the first report showing that the guest loading amount in NCPs can be tuned by the reaction temperature, which would be ascribed to the high coordination flexibility of lanthanide ions under different conditions.

SEM images (Figure 5) showed that the **D1**-loaded Gd−**L1**−**D1** NCPs prepared at both 20 and 140 °C (with slight aggregation) maintained the discus-like shape and the sizes are comparable with those of their corresponding bare Gd−**L1** NCPs. In addition, SAXRD analysis (Figure 5c) of Gd−**L1**−**D1** NCPs exhibited very similar reflection peaks with bare Gd−**L1** NCPs, which indicated that the guest doping did not influence the main skeleton of the coordination polymers. It is interesting that **D1**-loaded NCPs prepared at 140 °C can release the guest gradually when dispersed in DMF at room temperature. Approximately 82% of the encapsulated **D1** molecules can be released after 30 h. It should be noted that the guest encapsulation and release are reversible. The NCPs after release (collected by centrifugation) can re-encapsulate the guest molecules rapidly (in 5 min) at 140 °C if they are redispersed into the supernatant fluid of the reaction mixture. This novel mechanism of high-temperature fast loading and room-temperature slow release has great potential for drug delivery and controlled release systems.

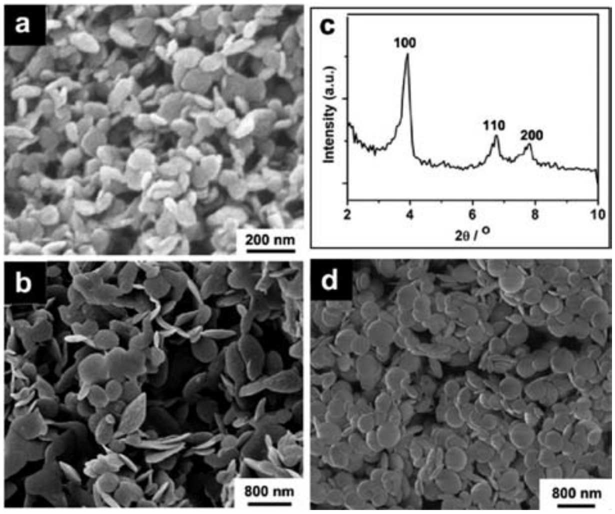

*Figure 5.* (a, b) SEM images of Gd−**L1**−**D1** NCPs prepared by coordination-directed assembly at 20 and 140 °C, respectively; (c) SAXRD data of the Gd−**L1**−**D1** sample shown in (b); (d) SEM image of Gd−**L1**−**D1** obtained by post-treatment of Gd−**L1** using **D1** at 140 °C. All of the samples were prepared in DMF and washed with ethanol before measurements.

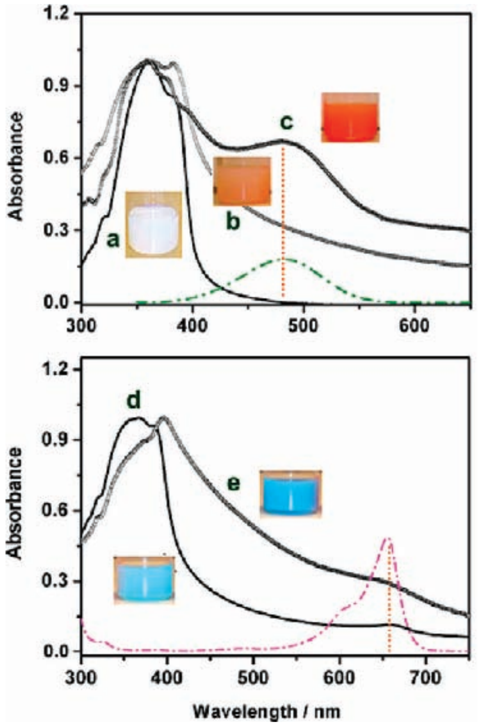

*Figure 4.* Normalized UV−vis absorption spectra of NCPs dispersed in ethanol: (a) Gd−**L1** prepared at 20 °C; (b) Gd−**L1**−**D1** prepared at 20 °C; (c) Gd−**L1**−**D1** prepared at 140 °C; (d) Gd−**L1**−**D2** prepared at 20 °C; (e) Gd−**L1**−**D2** prepared at 140 °C. The dashed curves are the absorptions of free **D1** and **D2** in ethanol, respectively. Inset: photograph of the corresponding NCPs dispersed in ethanol.

As the NCPs can re-encapsulate after release, the guest encapsulation is also expected by post-treatment of bare Gd−**L1** NCPs with **D1** at elevated temperatures. We found that, by the addition of **D1** into freshly prepared Gd−**L1** colloids at 140 °C, **D1** can be incorporated in 5 min while the particles maintain the original morphology and size, as revealed by SEM analysis (Figure 5d). The energy-dispersive X-ray (EDX) analysis of Gd−**L1**−**D1** nanoparticles prepared at 140 °C revealed the loss of iodine (Supporting Information). This indicated that the counteranion $I^-$ in **D1** was exchanged by another anion (most likely $CH_3COO^-$) in the self-assembly process. The presence of the acetate group was supported by two new peaks that arise at 1505 $cm^{-1}$ and 1380 $cm^{-1}$ in the IR spectrum. In addition, the stretching mode $\nu$(C=O) of coordinated DMF that peaked at 1659 $cm^{-1}$ disappeared due to the exchange by the acetate anion. To further investigate the temperature-controlled encapsulation mechanism, comparison experiments were also performed by post-treatment of purified Gd−**L1** NCPs with **D1** at 140 °C. Before post-treatment, the particles were collected by centrifugation and washed with ethanol, which was repeated four times to remove the free ligand and acetate anions. The experimental results showed that purified Gd−**L1** NCPs could not encapsulate **D1** molecules. These experimental results indicate that the negatively charged local environment around Ln(III) after binding of the acetate anion

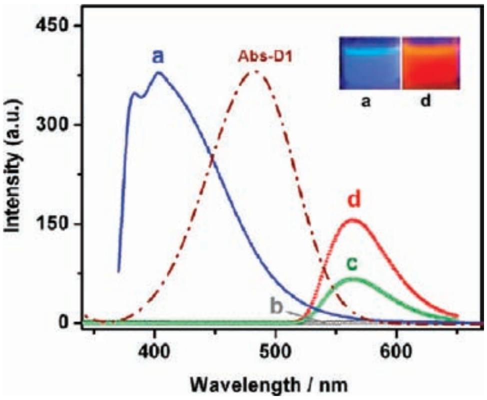

***Figure 6.*** PL spectra of **L1** (a), **L1** + **D1** (b), and **L1** + **D1** + Gd(OAc)$_3$ prepared at 20 °C (c) and 140 °C (d) in DMF. All of the samples have the same concentrations of **L1**; samples b, c, and d have the same concentration of **D1**. The dotted line is a UV−vis spectrum of **D1** in DMF. Inset: photo images of samples (a) and (d) under UV light (365 nm).

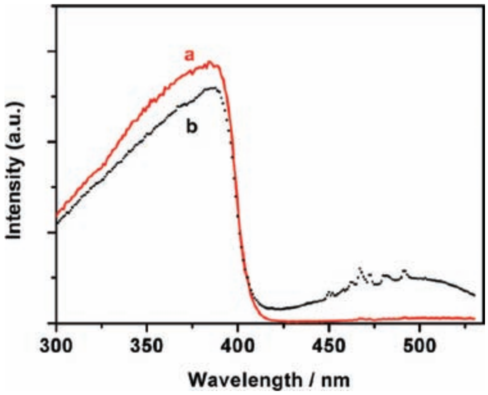

***Figure 7.*** Excitation spectra of Gd−**L1**−**D1** NCPs prepared at 20 °C (a) and 140 °C (b) after purification. The NCPs were dispersed in ethanol, and the emissions were detected at 600 nm.

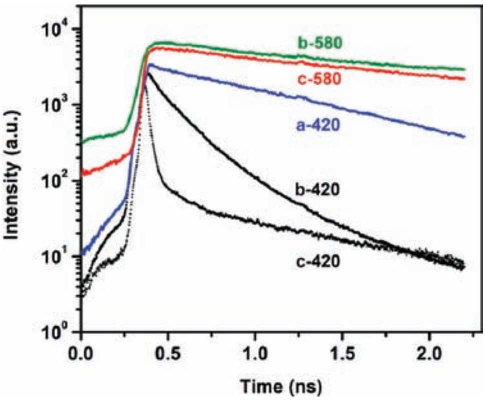

***Figure 8.*** Fluorescence decay profiles (Ex: 380 nm) of **L1** monitored at 420 nm (a-420); Gd−**L1**−**D1** sample prepared at 20 °C monitored at 420 nm (b-420) and 580 nm (b-580); and Gd−**L1**−**D1** sample prepared at 140 °C monitored at 420 nm (c-420) and 580 nm (c-580). All of the samples were dissolved or dispersed in ethanol.

is the driving force for the encapsulation of cationic guests. The temperature-controlled coordination-directed encapsulation mechanism is also suitable for other functional guests, such as **D2** (Figure 4d and 4e). The dye loading amount of **D2** is ∼2.8 mol% at 140 °C. The relatively lower loading concentration of **D2** is most likely due to the larger size of the three fused aromatic rings of the **D2** molecule compared to the linear **D1** molecule.

**Light-Harvesting Property.** The **D1**-loaded NCPs exhibit an efficient light-harvesting effect. In the present system, **L1** exhibits bright blue-violet emission ($\Phi = 0.98$ in DMF) while **D1** exhibits very weak emission due to efficient intramolecular charge transfer (ICT). The good overlap between the emission spectrum of **L1** (donor) and the absorption of **D1** (acceptor) favors the Förster-type energy transfer between them (Figure 6). However, when **L1** is mixed with **D1** in DMF with a molar ratio of 1:2, the strong emission of **L1** was quenched but no energy transfer emission could be observed. This indicates there is interaction between **L1** and **D1** and the quenching of the emission is most likely due to electron transfer or formation of nonfluorescent complexes.[23] Greatly enhanced emission at ∼580 nm appeared after further addition of Gd(OAc)$_3$ (Figure 6, inset). The excitation wavelength for the spectra here was 365 nm (the optimal excitation for **L1** but not for **D1**). It should be noted that even though the samples have the same concentrations of **L1**, **D1**, and Gd(OAc)$_3$, respectively, the NCPs prepared at 140 °C (Figure 6, curve d) exhibit apparently enhanced orange emission compared with the NCPs that were prepared at 20 °C (Figure 6, curve c). This indicates that the arrangement of **D1** in the nanometer-scaled matrix favors light harvesting.

The energy transfer was supported by the excitation spectra (Figure 7) of purified Gd−**L1**−**D1** NCPs prepared at 20 and 140 °C. The experiment results revealed that the emissions from the **D1** in NCPs are strongly enhanced by energy transfer from **L1** in the framework under excitation at 365 nm compared to direct excitation of the **D1** dye at 480 nm. Time-resolved fluorescence decay was also investigated to study the energy transfer process. As shown in Figure 8, the fluorescence lifetime of the free ligand **L1** detected at 420 nm (a-420) is 0.88 ns, which is shortened to 0.162 ns in Gd−**L1**−**D1** NCPs prepared at 20 °C (b-420), and even shorter 0.026 ns in the Gd−**L1**−**D1** NCPs prepared at 140 °C (c-420). The last value is close to the time resolution of the detection system. The lifetimes of the emission of the energy transfer, detected at 580 nm, are longer and on the order of 2.2 ns for the Gd−**L1**−**D1** NCPs prepared at both 20 °C (b-580) and 140 °C (c-580). There is a small but clearly observed delay in the buildup of the decay at 580 nm showing that they are not directly excited by the laser pulse.

The long-range ordered organization of photophysically active units at the supramolecular level on the nano- to micrometer scale is important in energy-transfer processes in photosynthetic systems, as well as electronic devices based on organic compounds.[24,25] Linear $\pi$-conjugated systems are especially relevant for this purpose, which play crucial roles in organic electronic devices, as the charge-transfer properties are strongly

---

(22) Auweter, H.; Haberkorn, H.; Heckmann, W.; Horn, D.; Lüddecke, E.; Rieger, J.; Weiss, H. *Angew. Chem., Int. Ed.* **1999**, *38*, 2188.

(23) (a) Vaiana, A. C.; Neuweiler, H.; Schulz, A.; Wolfrum, J.; Sauer, M.; Smith, J. C. *J. Am. Chem. Soc.* **2003**, *125*, 14564. (b) Liu, B.; Bazan, G. C. *J. Am. Chem. Soc.* **2006**, *128*, 1188. (c) Kaur, P.; Wu, M.; Anzaldi, L.; Waldeck, D. H.; Xue, C.; Liu, H. *Langmuir* **2007**, *23*, 13203. (d) Liu, M.; Kaur, P.; Waldeck, D. H.; Xue, C.; Liu, H. *Langmuir* **2005**, *21*, 1687. (e) Xu, Q.-H.; Moses, D.; Heeger, A. J. *Phys. Rev. B* **2003**, *67*, 245417.

(24) (a) Wasielewski, M. R. *Acc. Chem. Res.* **2009**, *42*, 1910. (b) Lim, Y.; Moon, K.-S.; Lee, M. *Chem. Soc. Rev.* **2009**, *38*, 925.

(25) (a) Ajayaghosh, A.; Vijayakumar, C.; Varghese, R.; George, S. J. *Angew. Chem., Int. Ed.* **2006**, *45*, 456. (b) Hoeben, F. J. M.; et al. *Angew. Chem., Int. Ed.* **2004**, *43*, 1976.

influenced by the long-range ordering of the conjugated chromophores.[25,26] Compared with the inefficient and costly covalent syntheses of large molecular arrays, self-assembly or supramolecular organization provides a facile mechanism for assembling large numbers of molecules into structures that can bridge length scales from nanometers to macroscopic dimensions.[24,27−29] Various elegant strategies have been followed to achieve organized multichromophoric light-harvesting antennae, such as organogels,[28] loading chromophores into microporous and mesoporous host materials[29] or organosilica structures,[30] dye-doped DNA nanofibers,[31] and other biomolecule-templated assemblies.[32] NCPs based light-harvesting materials reported here have considerable advantages for the design of a range of applications, such as photoreaction and light emitting with tunable emission wavelengths as the coordination-directed assembly can incorporate a variety of photoactive materials. For example, the energy transfer between **L1** and **D1** can be quenched by coloading **D1** and methylene blue (**D2**) into NCPs. This provides possibilities for the construction of more complicated photofunctional nanomaterials.

## Conclusions

In summary, we have demonstrated the coordination-directed organization of $\pi$-conjugated molecules into stable nanoparticle colloids with long-range ordered structures. These nanoscale coordination polymers exhibit temperature-controlled particle sizing, guest encapsulation, and release. The negatively charged local environment around the metal connector is the driving force for the encapsulation of cationic guests. Guest-loaded nanoparticles exhibit an efficient light-harvesting property. We envisage that this coordination-directed organization and encapsulation approach is general and should be extended to the fabrication of a wide range of multifunctional nanomaterials by judicious selection of the ligands, metal connectors, guests, and reaction mediums.

## Experimental Section

**Materials and Methods.** All of the chemicals were purchased from Sigma-Aldrich and used without further purification. The deionized (D.I.) water was generated using a Millipore Milli-Q system (Billerica, MA). MALDI-TOF (matrix-assisted laser desorption ionization time-of-flight) analysis was performed on a Bruker Autoflex II spectrometer. NMR analysis was performed on Bruker 300 and Bruker 400 instruments. UV−vis absorptions spectra of the NCPs were collected at room temperature on a UV-2450 UV−vis−NIR spectrophotometer with the samples dissolved/dispersed in ethanol. To determine the guest loading concentration, NCPs were digested using acetic acid and monitored by UV−vis absorption taking extinction coefficients (measured in acetic acid) into account. Fluorescence measurements were performed with a Fluoromax-4 spectrofluorometer at room temperature. The quantum efficiency ($\Phi_{fl}$) of **L1** in a dilute DMF solution was measured using quinine sulfate in 0.1 mol $L^{-1}$ sulfuric acid as a standard. IR spectra were collected on a Bruker Vertex 70 spectrometer (using KBr pellets) in the range 400−4000 $cm^{-1}$ (the magnified view from 700 to 1900 $cm^{-1}$ was shown in Figure S1). Small angle X-ray diffraction (SAXRD) measurements of the NCPs were performed using powdered samples on a Philips PW 1729 powder X-ray diffractometer (Cu K$\alpha$ radiation) over a 2$\theta$ range from 0.8° to 10°, and the data from 2° to 10° were shown in Figure 3. SEM images were obtained on an LEO 1550 FEG scanning electron microscope. Transmission electron microscopy (TEM) and EDX analysis were performed with an FEI Tecnai G2 microscope. The time-resolved fluorescence decay was investigated using 380 nm picosecond laser excitation and detected with a 0.5 m spectrometer equipped with a synchroscan streak camera. The time resolution is determined by the dispersion in the spectrometer and is typically 20 ps. The NCPs for fluorescence lifetime measurements were measured in an ethanol system. Before measurements, the NCPs were collected by centrifuge and redispersed in ethanol, which was repeated for four times to remove free molecules and metal ions.

**Preparation of NCPs.** All of the bared NCPs were prepared by a similar method using **L1** and different lanthanide acetates. Here, we use the preparation of Gd−**L1** as an example: **L1** (0.06 mmol, 37.3 mg) was dissolved in DMF (20 mL), and a $Gd(OAc)_3\cdot 4H_2O$ (0.04 mmol, 16.2 mg) solution dissolved in DMF (10 mL) was added dropwise under gentle stirring. The white colloid was stirred for 20 min and maintained at room temperature for different characterizations. SEM analysis revealed the particles are plate-shaped with diameters of 80−120 nm and thicknesses of 10−20 nm. NCPs with diameters of 500−600 nm can be obtained by increasing reaction temperatures to 140 °C with a reaction time of 20 min. Anal. Calcd (%) for Gd**L1**$_{1.5}\cdot$DMF$\cdot H_2O$: C, 68.73; H, 5.90; N, 1.19. Found (%): C, 68.70, H, 5.70; N, 0.80.

**Preparation of Gd−L1−D1 NCPs with Different D1 Loading Amounts.** All of the guest-loaded NCPs were prepared by a similar method using **L1** and different lanthanide acetates in the presence of guest molecules. Here, we use the preparation of Gd−**L1**−**D1** as an example: **L1** (0.06 mmol, 37.3 mg) and **D1** (0.12 mmol, 47.3 mg) were dissolved in DMF (30 mL), and a $Gd(OAc)_3\cdot 4H_2O$ (0.04 mmol, 16.2 mg) solution dissolved in DMF (10 mL) was added dropwise under gentle stirring. The mixture was stirred for 20 min (at 20, 80, or 140 °C) and then collected by centrifugation and washed with ethanol four times to remove free **L1** and **D1**. The **D1**-loaded NCPs can release guests gradually in DMF at room temperature but are stable in ethanol (does not release **D1** when it is dispersed in ethanol).

**Preparation of Gd−L1−D1 NCPs by Post-treatment of Gd−L1.** **L1** (0.06 mmol, 37.3 mg) was dissolved in DMF (20 mL) at 140 °C, and a $Gd(OAc)_3\cdot 4H_2O$ (0.04 mmol, 16.2 mg) solution

---

(26) (a) Hoeben, F. J. M.; Jonkheijm, P.; Meijer, E. W.; Schenning, A. P. H. J. *Chem. Rev.* **2005**, *105*, 1491. (b) Schenning, A. P. H. J.; Meijer, E. W. *Chem. Commun.* **2005**, 3245.

(27) (a) Cui, H.; Pashuck, T.; Velichko, Y. S.; Weigand, S. J.; Cheetham, A. G.; Newcomb, C. J.; Stupp, S. I. *Science* **2010**, *327*, 555. (b) Abbel, R.; van der Weegen, R.; Meijer, E. W.; Schenning, A. P. H. J. *Chem. Commun.* **2009**, 169.

(28) (a) Sugiyasu, K.; Fujita, N.; Shinkai, S. *Angew. Chem., Int. Ed.* **2004**, *43*, 1229. (b) Ajayaghosh, A.; Praveen, V. K. *Acc. Chem. Res.* **2007**, *40*, 644. (c) Ajayaghosh, A.; Praveen, V. K.; Vijayakumar, C.; George, S. J. *Angew. Chem., Int. Ed.* **2007**, *46*, 6260. (d) Ajayaghosh, A.; Praveen, V. K.; Srinivasan, S.; Varghese, R. *Adv. Mater.* **2007**, *19*, 411. (e) Ajayaghosh, A.; Vijayakumar, C.; Praveen, V. K.; Babu, S. S.; Varghese, R. *J. Am. Chem. Soc.* **2006**, *128*, 7174. (f) Praveen, V. K.; George, S. J.; Varghese, R.; Vijayakumar, C.; Ajayaghosh, A. *J. Am. Chem. Soc.* **2006**, *128*, 7542. (g) Vijayakumar, C.; Praveen, V. K.; Ajayaghosh, A. *Adv. Mater.* **2009**, *21*, 2059.

(29) (a) Calzaferri, G.; Huber, S.; Maas, H.; Minkowski, C. *Angew. Chem., Int. Ed.* **2003**, *42*, 3732. (b) Ruiz, A. Z.; Li, H.; Calzaferri, G. *Angew. Chem., Int. Ed.* **2006**, *45*, 5282. (c) Brühwiler, D.; Calzaferri, G.; Torres, T.; Ramm, J. H.; Gartmann, N.; Dieu, L.-Q.; López-Duarte, I.; Martínez-Díaz, M. V. *J. Mater. Chem.* **2009**, *19*, 804. (d) Wang, Y.; Li, H.; Feng, Y.; Zhang, H.; Calzaferri, G.; Ren, T. *Angew. Chem., Int. Ed.* **2010**, *49*, 1434. (e) Mech, A.; Monguzzi, A.; Meinardi, F.; Mezyk, J.; Macchi, G.; Tubino, R. *J. Am. Chem. Soc.* **2010**, *132*, 4574.

(30) Inagaki, S.; Ohtani, O.; Goto, Y.; Okamoto, K.; Ikai, M.; Yamanaka, K.; Tani, T.; Okada, T. *Angew. Chem., Int. Ed.* **2009**, *48*, 4042.

(31) Ner, Y.; Grote, J. G.; Stuart, J. A.; Sotzing, G. A. *Angew. Chem., Int. Ed.* **2009**, *48*, 5134.

(32) (a) Morikawa, M.; Yoshihara, M.; Endo, T.; Kimizuka, N. *J. Am. Chem. Soc.* **2005**, *127*, 1358. (b) Channon, K. J.; Devlin, G. L.; MacPhee, C. E. *J. Am. Chem. Soc.* **2009**, *131*, 12520. (c) Kumar, C. V.; Fuff, M. R. *J. Am. Chem. Soc.* **2009**, *131*, 16024. (d) Miller, R. A.; Presley, A. D.; Francis, M. B. *J. Am. Chem. Soc.* **2007**, *129*, 3104. (e) Nam, Y. S.; Shin, T.; Park, H.; Magyar, A. P.; Choi, K.; Fantner, G.; Nelson, K. A.; Belcher, A. M. *J. Am. Chem. Soc.* **2010**, *132*, 1462.

dissolved in DMF (10 mL) was added dropwise under stirring. The white colloid was stirred for 20 min at 140 °C, a solution of **D1** (0.12 mmol, 47.3 mg) in DMF (10 mL) was added, and the mixture was stirred for 5 min. The red powder was collected by centrifugation and washed with ethanol to remove free **L1** and **D1**.

**Acknowledgment.** We acknowledge the support from the Swedish Foundation for Strategic Research (SSF) within the Nano-X program (Grant No. SSF [A3 05:204]). We thank Dr. Shankara Narayanan for helpful discussions and Mr. Thomas Lingefelt for SEM measurement.

**Supporting Information Available:** Experimental details, synthetic procedures for the ligand, characterization data, and complete refs 13a and 25b. This material is available free of charge via the Internet at http://pubs.acs.org.

JA102299B